doi:10.1111/j.1558-5646.2008.00507.x

RAPID COLOR EVOLUTION IN AN APOSEMATIC SPECIES: A PHYLOGENETIC ANALYSIS OF COLOR VARIATION IN THE STRIKINGLY POLYMORPHIC STRAWBERRY POISON-DART FROG

Ian J. Wang[1,2] and H. Bradley Shaffer[1]

[1]*Department of Evolution and Ecology and Center for Population Biology, University of California, Davis, California 95616*

[2]*E-mail: ijwang@ucdavis.edu*

Received March 28, 2008
Accepted August 6, 2008

Aposematism is one of the great mysteries of evolutionary biology. The evolution of aposematic coloration is poorly understood, but even less understood is the evolution of polymorphism in aposematic signals. Here, we use a phylogeographic approach to investigate the evolution of color polymorphism in *Dendrobates pumilio*, a well-known poison-dart frog (family Dendrobatidae), which displays perhaps the most striking color variation of any aposematic species. With over a dozen color morphs, ranging from bright red to dull green, *D. pumilio* provides an ideal opportunity to examine the evolution of color polymorphism and evolutionary shifts to cryptic coloration in an otherwise aposematic species. We constructed a phylogenetic tree for all *D. pumilio* color morphs from 3051bp of mtDNA sequence data, reconstructed ancestral states using parsimony and Bayesian methods, and tested the recovered tree against constraint trees using parametric bootstrapping to determine the number of changes to each color type. We find strong evidence for nearly maximal numbers of changes in all color traits, including five independent shifts to dull dorsal coloration. Our results indicate that shifts in coloration in aposematic species may occur more regularly than predicted and that convergence in coloration may indicate that similar forces are repeatedly driving these shifts.

KEY WORDS: **Amphibian, morphological radiation, phylogeography, warning signal.**

Aposematic coloration is a perplexing phenomenon (Mallet and Joron 1999; Rowe and Guilford 2000; Santos et al. 2003; Merilaita and Tullberg 2005). Although the benefit of predator deterrence likely exists once a warning signal establishes itself in a species, theory predicts that the probability of establishment should be low because of an increased probability of predation at low initial frequencies (Yachi and Higashi 1998; Servedio 2000; Santos et al. 2003; Speed and Ruxton 2005; Puurtinen and Kaitala 2006). Polymorphism in aposematic coloration is even more perplexing (Harvey et al. 1982; Endler 1988; Joron et al. 1999; Darst and Cummings 2006; Reynolds and Fitzpatrick 2007) because individual fitness should behave according to the expectations of Müllerian mimicry (Guilford and Dawkins 1993; Endler and Mappes 2004) such that any individual that deviates from a predator-recognized "warning" coloration incurs an increased risk of predation (Muller 1879; Benson 1972). Thus, the a priori expectation is that color and pattern should be heavily constrained in aposematic species (Harvey et al. 1982; Endler 1988; Darst and Cummings 2006; Reynolds and Fitzpatrick 2007). However, there have been few explicit tests of this prediction.

Phylogenetic analyses of character evolution are a key component to our understanding of phenotypic polymorphism in aposematic species. In particular, understanding the evolutionary history of populations that vary widely in aposematic traits

is critical for formulating predictions and assumptions about the forces that are likely to constrain or facilitate the evolution of these traits. For example, normalizing selection is expected to remove variation in aposematic traits (Muller 1879; Benson 1972; Guilford and Dawkins 1993; Endler and Mappes 2004), suggesting that transformations between alternate aposematic states, or the rapid gain and loss of aposematic coloration, should be uncommon events.

The greatest power to quantitatively examine the evolution of aposematic traits will come from taxa having a large number of substantially differentiated color morphs, because they yield the greatest potential for observing character state transformations within species. Only a few species fit this criterion. One particularly compelling species for studying aposematic color evolution in this context is *Dendrobates pumilio*, the strawberry poison-dart frog, which displays perhaps the most striking color polymorphism of any amphibian (Daly and Myers 1967; Savage 2002). Dendrobatid frogs, known for their bright coloration and unique system of toxin secretory glands, provide some of the most conspicuous and well-studied examples of color aposematism (Summers and Clough 2001; Savage 2002; Santos et al. 2003; Vences et al. 2003). Among dendrobatid frogs, *D. pumilio* displays a particularly striking level of color variation (Myers and Daly 1983; Summers et al. 1997; Hoffman and Blouin 2000).

Populations of *D. pumilio* are composed of a single, aposematic color morph throughout most of the species' range from central Panama to northern Nicaragua (Savage 2002; Saporito et al. 2007). These frogs are bright red with dull blue/black limbs and limited dark spotting on the dorsum (Fig. 1, La Selva). However, in a small region in northwestern Panama, the Bocas del Toro archipelago, *D. pumilio* exhibits a wide array of colors, including bright colors such as red and orange and duller colors like green and blue (Fig. 1; Table 1; Myers and Daly 1983; Summers et al. 1997; Summers et al. 2003; Summers et al. 2004). Although there is substantial phenotypic variation among populations, no sexual dimorphism is apparent (Summers et al. 1997; Savage 2002; Reynolds and Fitzpatrick 2007; Rudh et al. 2007). Color morphs are generally allopatric, with one morph inhabiting each island

Figure 1. Dorsal (left) and ventral (right) views of exemplars from each sampled population of *Dendrobates pumilio* in Costa Rica and Panama.

Table 1. Character traits for color morphs in the Bocas del Toro clade. Populations are listed with their normal dorsal coloration, ventral coloration, and spotting pattern. Variation within populations is typically minimal, with the exception of Uyama River, which is found in the Bocas del Toro region but not in the Bocas del Toro clade, and Bastimentos, which has morphs with red, orange, and yellow dorsal coloration.

Population	Dorsal	Ventral	Pattern
Guabo River	green	yellow	speckled
Colon	green	yellow	spotted
Agua	green	yellow	solid
Pastores	green-brown	yellow-brown	speckled
Cerro Brujo	blue	blue	solid
Popas	green	yellow	solid
Solarte	red-orange	red-orange	solid
Almirante	red-orange	red-orange	solid
San Cristobal	red	red	speckled
Bastimentos	red/orange/yellow	white	spotted
Puerto Viejo	red	red	speckled

(Fig. 2). In general, little phenotypic variation exists within populations compared to that between Bocas del Toro populations (Summers et al. 1997; Reynolds and Fitzpatrick 2007).

The polymorphism in *D. pumilio* is striking not just because of the degree of variation but also because the geological events creating these islands occurred within the last 1000–10,000 years (Fig. 3; Anderson and Handley 2002), suggesting that the observed among-island variation in *D. pumilio* may have arisen quite rapidly (Summers et al. 1997). Several adjacent mainland localities also contain divergent color morphs even though these areas are part of generally contiguous tracts of suitable habitat along the Caribbean coast of Central America. Consistent with this observation, several biogeographic studies of other amphibians have detected a "Bocas break" where lineages show substantial genetic divergence on either side of the Bocas del Toro region in spite of no obvious geographic barrier (Crawford et al. 2007; Wang et al. 2008).

Several explanations for this observed color polymorphism in *D. pumilio* have been proposed, including sexual selection (Summers et al. 1997, 1999; Reynolds and Fitzpatrick 2007; Rudh et al. 2007), natural selection (Daly and Myers 1967; Reynolds and Fitzpatrick 2007; Rudh et al. 2007), and random drift (Daly and Myers 1967; Reynolds and Fitzpatrick 2007). Two studies have shown that females prefer mates of their own color morph (Summers et al. 1999; Reynolds and Fitzpatrick 2007), although the extent to which sexual selection has driven the evolution of novel color morphs instead of reinforcing the reproductive isolation of morphs remains unclear. Summers et al. (1997) provide evidence that neutral divergence alone is unlikely to have caused the variation in color patterns, although Daly and Myers (1967) and Rudh et al. (2007) argue that reduced population sizes associated with island colonizations were likely to have played some role in the fixation of novel phenotypes. Clearly, sorting out the extent to which each of these forces has driven color variation in *D. pumilio* remains an active area of investigation, and future studies would likely benefit from a strongly supported phylogenetic history of the color morphs under consideration.

Several phylogenetic hypotheses for the relationships of *D. pumilio* populations in the Bocas del Toro archipelago have been proposed. Summers et al. (1997) generated the first such phylogeny from 292bp of mtDNA sequence data sampled from one mainland and five island populations. More recently, Hagemann and Prohl (2007) compiled a tree based on 1215bp of mtDNA sequence data for single exemplars from all islands and two mainland localities and Rudh et al. (2007) presented a dendrogram for all but one island population and a single mainland population based on AFLP markers. All three of these analyses are important steps in understanding the relationships of color morphs in *D. pumilio*, although none offers completely satisfying solutions to this complex problem. The phylogenies generated by Summers et al. (1997) and Rudh et al. (2007) were both relatively unresolved in terms of nodal support, suggesting that this has been a recent evolutionary radiation. The dendrogram of Rudh et al. (2007) is further complicated by the inherent difficulties of inferring phylogeny from distance-based analyses of genotypic data (Zink and Barrowclough 2008) and potentially by the effects of demographic history (both of which are acknowledged in the study). The phylogeny from Hagemann and Prohl (2007), although statistically well-supported, provides limited information because only single haplotypes were sampled from each population; sampling multiple individuals per population is necessary to distinguish interpopulation divergence from within-population variation. Finally, all of these studies omit some of the color morphs in the Bocas del Toro region, and, therefore, present tantalizing, but incomplete insights into this radiation. Thus, despite the number of intriguing evolutionary questions that have been examined in this system, we still lack a fully resolved framework for understanding the evolutionary relationships of color morphs and for determining the history of color and pattern changes in the group.

Here, we present a phylogenetic analysis of color evolution in *D. pumilio*, using both much longer sequences of mtDNA and more complete population sampling than previous phylogenetic analyses. Like Summers et al. (1997) and Hagemann and Prohl (2007), we base our results solely on mtDNA, and we briefly review the difficulties inherent in this strategy. However, both the biology of the frogs and comparisons with published and unpublished nuclear results suggest that our resulting mtDNA tree is probably a reasonable representation of population history for *D. pumilio*. We use this phylogeny to resolve the history of color pattern transformations in *D. pumilio* from the Bocas del Toro

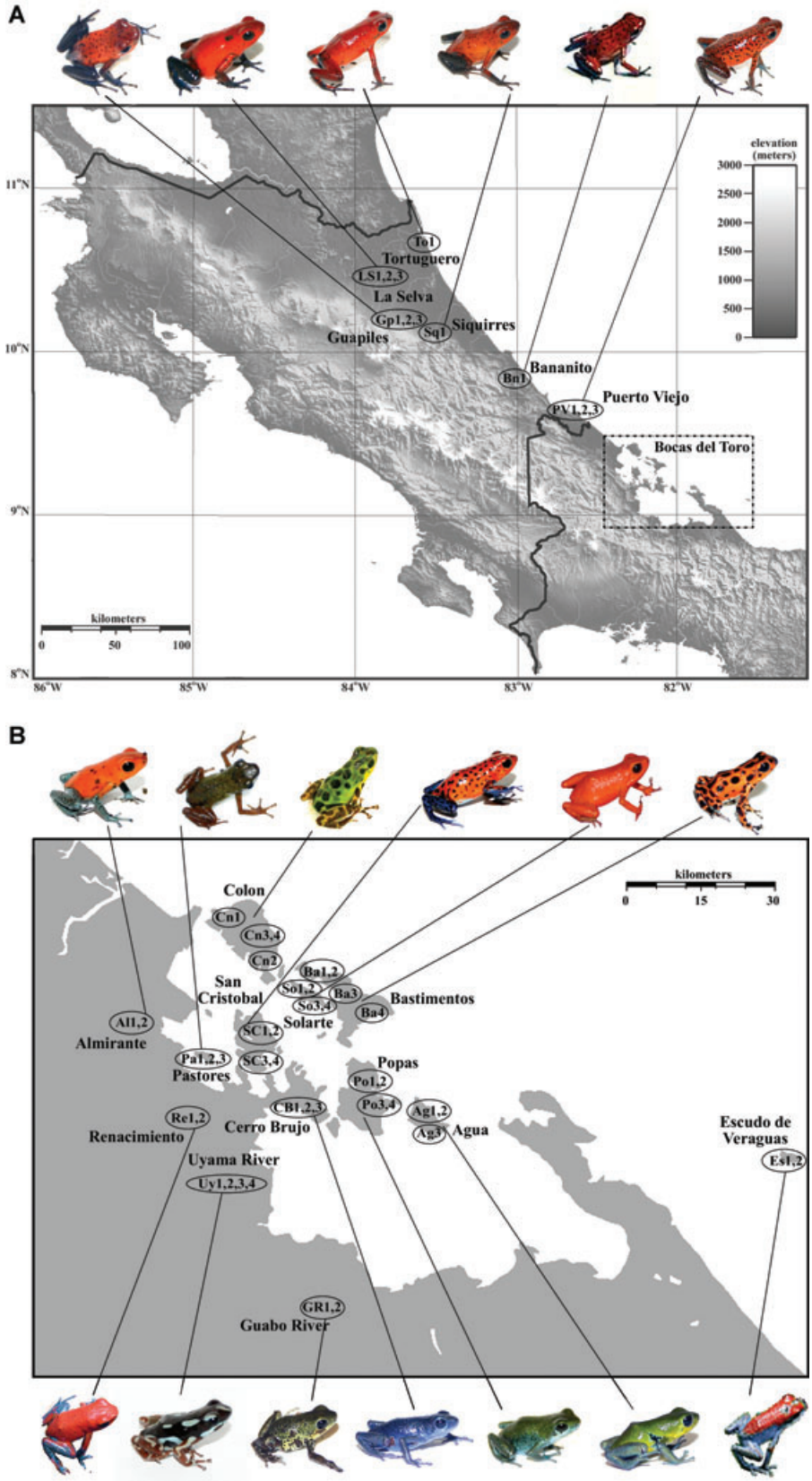

Figure 2. Collection localities for *Dendrobates pumilio* tissues used in phylogenetic analysis. Labels within ellipses reference the sample acronyms used in Table 2. Map (A) shows collection localities in Costa Rica. The dashed box outlines the Bocas del Toro region, which is enlarged in map (B) with collection localities in Panama. Exemplars of each morph are shown for each locality.

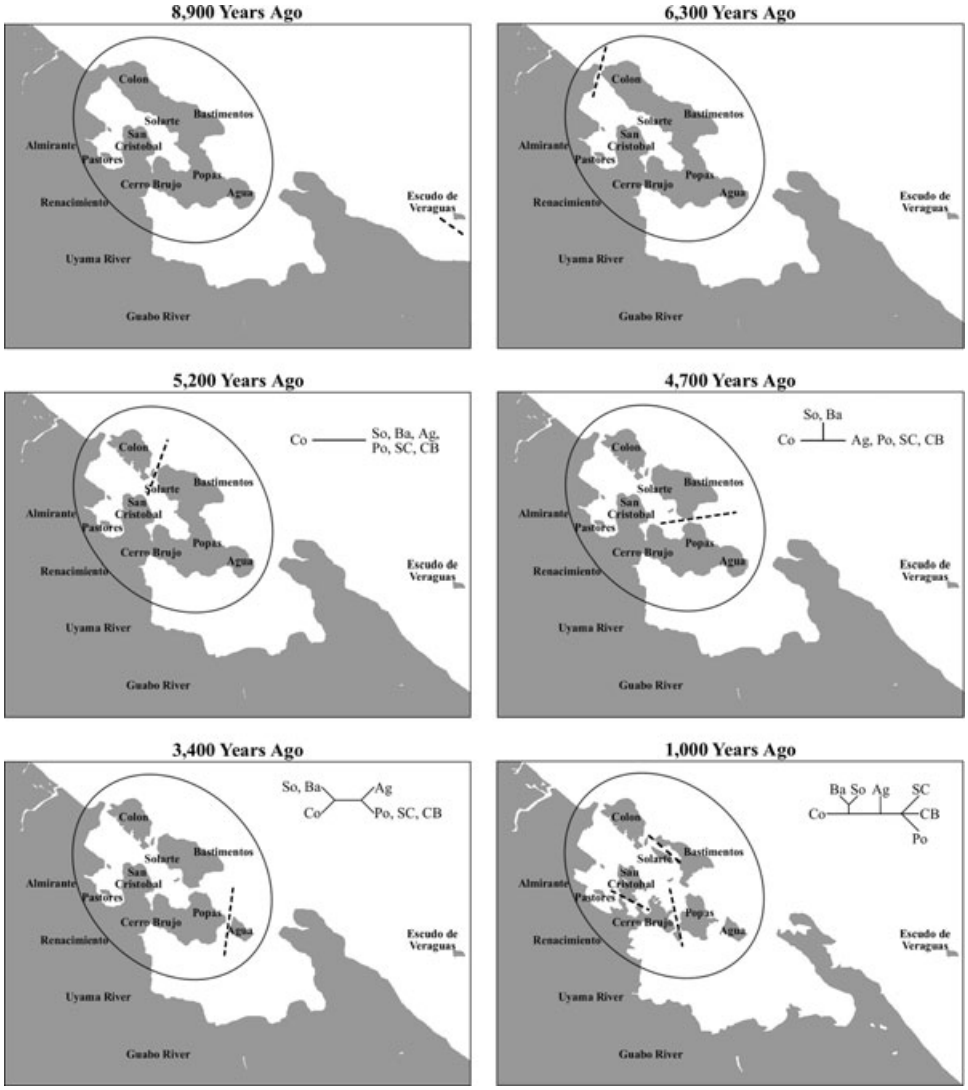

Figure 3. **Reconstructed history of island isolation in the Bocas del Toro archipelago, based on Anderson and Handley (2002). Individual panels show the configuration of islands and mainland peninsulas at 8900, 6300, 5200, 4700, 3400, and 1000 years ago. Each panel also includes a cladogram showing the topological relationships predicted by a vicariance model of sequential island isolation at each point in time. The cladogram from 1000 years ago (bottom-right) was used as an a priori null hypothesis constraint tree in a SOWH test to determine whether the relationships of current populations are exclusively the result of vicariance.**

archipelago. Our primary objectives were to determine (1) the history of the phenotypically variable populations in the Bocas del Toro region, (2) the phylogenetic relationships among different color morphs, (3) the number of evolutionary changes to each color and spotting pattern among Bocas del Toro populations, and (4) whether convergent evolution has played a significant role in generating similarly colored morphs on different islands.

Materials and Methods

STUDY SYSTEM: THE FROGS

Dendrobates pumilio is a small, diurnal, lowland wet-forest frog. The species occurs throughout eastern Nicaragua and Costa Rica and into northern Panama. Like many dendrobatid frogs, most populations of *D. pumilio* are extremely toxic (Daly and Myers 1967). Toxins in skin secretions are dietarily derived from small arthropods, primarily formicine ants (Daly and Myers 1967; Saporito et al. 2004), which form the bulk of their diet.

There are two exceptions to the observation of little intrapopulation color variation. The island of Bastimentos harbors three morphs: red, orange, and yellow (Fig. 1), with yellow being rare. Also, the mainland Uyama river population is highly polymorphic, with individuals having stripes of variable lengths and colors, including light blue, yellow, and red, on a black dorsum (Fig. 1). In both cases variation is only present on the dorsum, and ventral surfaces are relatively constant.

STUDY SYSTEM: THE LANDSCAPE

The Bocas del Toro archipelago is located along the Caribbean coast of northwestern Panama. Islands in the archipelago formed during the Holocene when rising sea levels and continental submergence isolated hills and ridges (Olson 1993; Anderson and Handley 2002). Based primarily on historical estimates of sea levels and current ocean-floor topography, Anderson and Handley (2002) reconstructed the sequence of island isolation in the archipelago (Fig. 3). Escudo de Veraguas was the first island to separate from the mainland, approximately 8900 years ago, and this island is currently well east of the main island chain. The remaining islands separated sequentially from a peninsula that was formed when present-day Colon separated from Almirante 6300 years ago. Colon was isolated as an island when it separated from the peninsula 5200 years ago, followed by Bastimentos 4700 years ago, and Agua 3400 years ago. Within the past 1000 years, San Cristobal and Popas each separated from the mainland peninsula, and Solarte and Bastimentos split to form separate islands.

SAMPLE COLLECTION

We collected tissue samples via toe-clip from 19 localities: six in Costa Rica and 13 in the Bocas del Toro region of Panama (Fig. 2; Table 2). Samples were taken from several points on each of the islands in Bocas del Toro (Fig. 2B; Table 2) and were immediately preserved in 95% ethanol. Photographs were taken of each sampled animal with a Canon EOS 300D digital camera (Canon U.S.A., Inc., Lake Success, NY). To facilitate color standardization, each frog was placed on a solid white background with an RGB color correction grid. The grid contains red, green, and blue squares to provide three calibration points along the major axes in an RGB color system. We also sampled single specimens of *D. tinctorius* and *D. auratus*, which are putative sisters to the *histrionicus* group of which *D. pumilio* is a member (Vences et al. 2003; Grant et al. 2006; Roberts et al. 2006), to serve as outgroup taxa.

DNA SEQUENCING

Tissues were digested in lysis buffer with Proteinase K, and genomic DNA was purified using a standard ethanol precipitation. Extracted samples were diluted to 10 ng/μl and used as template in PCR reactions for four mtDNA regions (CytB, COI, ND4, and control region) using the primers and annealing temperatures provided in Table 3. Amplified fragments were sequenced in both directions using PCR primers, plus one set of internal primers, and Big Dye 3.1 dye-terminator cycle sequencing reaction chemistry, and were analyzed on an ABI 3730 capillary electrophoresis genetic analyzer (Applied Biosystems, Foster City, CA) at the UC Davis College of Biological Sciences DNA Sequencing Facility (http://dnaseq.ucdavis.edu/). DNA sequences were aligned with Sequencher version 4.2 (Gene Codes Corporation, Ann Arbor, MI), and resulting sequences were uploaded to GenBank (accession numbers EU934546-EU934733).

PHYLOGENETIC ANALYSIS

We concatenated sequences for each individual, and calculated nucleotide variation within populations and net divergence between populations in MEGA version 4.0.26 (Tamura et al. 2007), using the Tamura and Nei (1993) nucleotide substitution model, equal rates of substitution among lineages, rate variation among sites ($\gamma = 0.5$), and estimating standard errors from 500 bootstrap replicates. We performed maximum likelihood (ML) analyses (Felsenstein 1981) using PAUP* version 4.0b10 (Swofford 2001). We used Modeltest version 3.6 (Posada and Crandall 1998) to evaluate 56 potential models of DNA sequence evolution and chose the most appropriate model by the AIC. We used heuristic searches to estimate the ML phylogenetic tree starting from a neighbor-joining (NJ) tree (Saitou and Nei 1987) with TBR branch swapping. Trees were rooted with *D. tinctorius* and *D. auratus* as outgroups. We assessed statistical support for ML clades with nonparametric bootstrap analysis (Felsenstein 1985) using 500 bootstrap replicates, each having one random addition sequence replicate and TBR branch swapping.

We conducted a Bayesian MCMC (Rannala and Yang 1996; Yang and Rannala 1997) phylogenetic analysis using MrBayes version 3.1.2 (Huelsenbeck and Ronquist 2001). We partitioned our dataset into four individual gene regions, assumed a separate model of evolution for each partition, and allowed the partitions to evolve under different rates. We conducted one run with 10 million generations sampled every 500 generations with four Metropolis-coupled MCMC chains using default heating ($T = 0.2$), evaluated the resulting collection of trees for convergence by examining the standard deviation of split frequencies, and discarded all preburnin trees obtained before the run achieved a stationary state. We estimated the posterior probability distribution of topologies, branch lengths, and parameter values from the combined 7012 samples of postburnin trees.

Because incomplete lineage sorting has the potential to confound phylogenetic analyses of recently diverged populations, we also performed the "minimize deep coalescences method" following the procedure of Maddison and Knowles (2006). This method takes into account the process of lineage sorting by genetic drift and information on the genealogical relationships among alleles (Maddison and Knowles 2006) and has been shown to improve the probability of recovering an accurate population tree, even with a single locus (Knowles and Carstens 2007). We first performed a parsimony analysis in PAUP*, using a heuristic search with 1000 random addition sequence replicates and maxtrees = 100, and saved a majority-rule consensus tree from all equally parsimonious trees recovered in the search. We then used the tree search tool in Mesquite version 2.5 (Maddison and Maddison 2005) to

Table 2. Tissue samples from which DNA sequences used in phylogenetic analysis were obtained. Specimen data include the acronym designation used in Figures 3 and 4, the population designation, the province and country in which the population is found, and the latitudinal and longitudinal coordinates at which the specimen was collected.

Sample	Population	Province, Country	Latitude	Longitude
Cn1	Colon	Bocas del Toro, Panama	9.4206	−82.3092
Cn2	Colon	Bocas del Toro, Panama	9.3652	−82.2507
Cn3	Colon	Bocas del Toro, Panama	9.4006	−82.2663
Cn4	Colon	Bocas del Toro, Panama	9.4006	−82.2663
Ba1	Bastimentos	Bocas del Toro, Panama	9.3451	−82.2015
Ba2	Bastimentos	Bocas del Toro, Panama	9.3451	−82.2015
Ba3	Bastimentos	Bocas del Toro, Panama	9.3115	−82.1437
Ba4	Bastimentos	Bocas del Toro, Panama	9.2987	−82.1044
Pa1	Pastores	Bocas del Toro, Panama	9.2369	−82.3384
Pa2	Pastores	Bocas del Toro, Panama	9.2369	−82.3384
Pa3	Pastores	Bocas del Toro, Panama	9.2369	−82.3384
Al1	Almirante	Bocas del Toro, Panama	9.2675	−82.4023
Al2	Almirante	Bocas del Toro, Panama	9.2675	−82.4023
SC1	San Cristobal	Bocas del Toro, Panama	9.2600	−82.2843
SC2	San Cristobal	Bocas del Toro, Panama	9.2600	−82.2843
SC3	San Cristobal	Bocas del Toro, Panama	9.2410	−82.2692
SC4	San Cristobal	Bocas del Toro, Panama	9.2410	−82.2692
CB1	Cerro Brujo	Bocas del Toro, Panama	9.1831	−82.2211
CB2	Cerro Brujo	Bocas del Toro, Panama	9.1831	−82.2211
CB3	Cerro Brujo	Bocas del Toro, Panama	9.1831	−82.2211
So1	Solarte	Bocas del Toro, Panama	9.3260	−82.2112
So2	Solarte	Bocas del Toro, Panama	9.3260	−82.2112
So3	Solarte	Bocas del Toro, Panama	9.3140	−82.1926
So4	Solarte	Bocas del Toro, Panama	9.3140	−82.1926
GR1	Guabo River	Bocas del Toro, Panama	8.8876	−82.2058
GR2	Guabo River	Bocas del Toro, Panama	8.8876	−82.2058
Po1	Popas	Bocas del Toro, Panama	9.1833	−82.1378
Po2	Popas	Bocas del Toro, Panama	9.1833	−82.1378
Po3	Popas	Bocas del Toro, Panama	9.1745	−82.1072
Po4	Popas	Bocas del Toro, Panama	9.1745	−82.1072
Ag1	Agua	Bocas del Toro, Panama	9.1634	−82.0367
Ag2	Agua	Bocas del Toro, Panama	9.1634	−82.0367
Ag3	Agua	Bocas del Toro, Panama	9.1502	−82.0375
Re1	Renacimiento	Bocas del Toro, Panama	9.1815	−82.3434
Re2	Renacimiento	Bocas del Toro, Panama	9.1815	−82.3434
Uy1	Uyama River	Bocas del Toro, Panama	9.0004	−82.3022
Uy2	Uyama River	Bocas del Toro, Panama	9.0004	−82.3022
Uy3	Uyama River	Bocas del Toro, Panama	9.0004	−82.3022
Uy4	Uyama River	Bocas del Toro, Panama	9.0004	−82.3022
Es1	Escudo de Veraguas	Bocas del Toro, Panama	9.0943	−81.5646
Es2	Escudo de Veraguas	Bocas del Toro, Panama	9.0943	−81.5646
PV1	Puerto Viejo	Limon, Costa Rica	9.6500	−82.7600
PV2	Puerto Viejo	Limon, Costa Rica	9.6500	−82.7600
PV3	Puerto Viejo	Limon, Costa Rica	9.6500	−82.7600
Sq1	Siquirres	Limon, Costa Rica	10.0930	−83.4970
Bn1	Bananito	Limon, Costa Rica	9.8240	−83.0630
To1	Tortuguero	Limon, Costa Rica	10.5680	−83.5190
Gp1	Guapiles	Sarapiqui, Costa Rica	10.2060	−83.7970
Gp2	Guapiles	Sarapiqui, Costa Rica	10.2060	−83.7970
Gp3	Guapiles	Sarapiqui, Costa Rica	10.2060	−83.7970
LS1	La Selva	Sarapiqui, Costa Rica	10.4290	−84.0070
LS2	La Selva	Sarapiqui, Costa Rica	10.4290	−84.0070
LS3	La Selva	Sarapiqui, Costa Rica	10.4290	−84.0070

Table 3. Primers used in PCR and sequencing reactions. Primers are listed in the pairs used in PCR with the gene amplified, primer name, primer sequence, and annealing temperature (T_A) in degrees Celsius. Primers DpumCR-L4 and DpumCR-H4 were only used in sequencing reactions, so do not have annealing temperature listed.

Gene	Primer	Sequence	T_A	Reference
ND4	ND4L	5′- TGACTACCAAAAGCTCATGTAGAAGC -3′	48	Arevalo et al. (1994)
	ND4-1	5′- GAAAGTGTTTAGCTTTCATCTCTAG -3′		Burns et al. (2007)
COI	LCO1490	5′- GGTCAACAAATCATAAAGATATTGG -3′	50	Folmer et al. (1994)
	HCO2198	5′- TAAACTTCAGGGACCAAAAAATCA -3′		Folmer et al. (1994)
CytB	DpumCB-L2	5′- GCCTTCTCCTCCAGCCCAC -3′	64	This study.
	cytbAR-H	5′- TAWAAGGGTCTTCTACTGGTTG		Goebel et al. (1999)
control region	CytbA-L	5′- GAATYGGRGGWCAACCAGTAGAAGACCC -3′	64	Goebel et al. (1999)
	ControlP-H	5′- GTCCATAGATTCASTTCCGTCAG -3′		Goebel et al. (1999)
	DpumCR-L4	5′- CCCCCATCTTTTCTTCTCCT -3′		This study.
	DpumCR-H4	5′- GATCAGGATCTGTTGGGGAA -3′		This study.

find the population tree that minimized the total number of deep coalescences, using the saved majority-rule consensus tree and SPR branch swapping (Maddison and Knowles 2006).

CLUSTERING OF TRAITS

Comparisons of coloration are inherently difficult. Color exists on a continuum, but colors also form classes that are commonly recognizable. Despite the wide range of variation in *D. pumilio* (Fig. 1), coloration may fall into discrete categories. *Dendrobates pumilio* morphs display a mix of colors, including bright colors typically associated with aposematism (red, orange, and yellow) and dull colors typically associated with crypsis (green and brown). Dull coloration (brown) has been shown to result in increased predation compared to bright colors in experimental models (Saporito et al. 2007), and dull colors are generally more difficult for potential predators to distinguish from backgrounds (Norris and Lowe 1964; Siddiqi et al. 2004), suggesting a significant ecological difference in these two colors classes. Likewise, ventral colors appear to fall into discrete categories including red, yellow, white, blue, and green (Fig. 1; Table 1). Some evidence from quantitative analysis of color variation among populations indicates that the range of colors expressed by *D. pumilio* has a discontinuous distribution (Rudh et al. 2007). Additionally, color expression is controlled by the synthesis of particular pigment molecules (Summers et al. 2003). Thus, both the discontinuous variation measured in *D. pumilio* coloration and the proximate mechanism underlying color expression imply that color in *D. pumilio* is best treated as a series of unordered, qualitative trait values rather than as a continuous quantitative trait. In this sense, frog coloration is akin to human eye color; green eyes are not intermediate between blue and brown, nor is yellow a necessary step between green and orange frogs.

To investigate whether dorsal and ventral colors from each population form discrete classes and to examine convergence in coloration, we performed *k*-means clustering (Hartigan and Wong 1979) on color characters. We used ImageJ version 1.37 (Abramoff et al. 2004) to measure the strengths of red, green, and blue (RGB) at 15 randomly chosen points on each of the dorsal and ventral surfaces of 20 field-collected individuals from each population in a method similar to previous studies of coloration in dendrobatid frogs (Roberts et al. 2006; Rudh et al. 2007). We then plotted the mean of each population on a three-dimensional graph with RGB axes.

Under *k*-means clustering, an iterative process determines the membership of each cluster. *k* centroids are placed into the space occupied by the sample points, and each sample point is assigned to a cluster represented by the nearest centroid based upon Euclidean distance. A new centroid is then calculated by finding the center of the resulting cluster, and the process is repeated until centroids no longer change coordinates (Hartigan and Wong 1979). We performed the analysis 1000 times for $k = 1$ to $k = 5$, randomly assigning initial centroids RGB values within the ranges of the values contained in our samples for each test.

The two major challenges of *k*-means clustering are determining the membership of clusters and identifying the appropriate number of clusters contained in the data (Gordon 1999; Tibshirani et al. 2001). Using multiple iterations with random starting points is a technique that addresses both challenges (Gordon 1999). Because the resulting membership of clusters can be affected by the placement of initial centroids, randomly placing initial centroids avoids bias in centroid selection. Using multiple iterations minimizes stochastic effects; initial centroid placement is still random, but choosing many random initial points reduces sampling error. Additionally, through multiple iterations, we can also assess the consistency with which particular clusters are recovered (Hartigan and Wong 1979; Gordon 1999). Clusters should be recovered with high consistency if sets of points are well differentiated in space, because the initial starting position of centroids will affect the

membership of clusters less than the inherent spatial structure of color points.

We took steps to compensate for any distortion in color caused by the use of a digital camera, including using a high-quality camera and lens system, standardizing with a color correction grid, and shooting in a RAW image file format that retains more color information than compressed images. Together, these should allow us to make relative comparisons of coloration (Rudh et al. 2007; Stevens et al. 2007). As a further check, we also extracted data from a previously published study of spectral reflectance in *D. pumilio*, measured by spectrometer (Summers et al. 2003). We identified the wavelength corresponding to the spectral peak in each of the spectral reflectance graphs presented in that study, averaged results for each color morph, and performed one-dimensional *k*-means clustering for the resulting wavelength measurements.

In addition to color shades, morphs are also distinguished by spotting patterns. Patterns were classified as either "spotted," "speckled," or "solid." Spotted pattern indicates the presence of several large, round dark pigment regions, whereas speckled indicates the presence of many small, irregular marks. For example, Bastimentos and Colon are spotted, Siquirres is speckled, and Solarte is solid (Fig. 1).

Finally, it is undoubtedly the case that the perception of color is as ecologically important as the expression of color, and so human perception of frog coloration may vary from that of potential predators. There are few observations of predation events in the wild, but birds are generally presumed to by the major predator of *D. pumilio* (Myers and Daly 1983; Siddiqi et al. 2004). Although birds have tetrachromatic vision (four cones) whereas humans are trichromatic, their visible spectrum (320–700 nm) is similar to that of humans (380–750 nm), shifted only slightly toward ultraviolet wavelengths (Vorobyev et al. 1998; Endler and Mielke 2005). Summers et al. (2003) demonstrated that most reflectance spectra from the Bocas del Toro color morphs peak between 400 and 700 nm and that reflectance spectra tend to have single peaks. Thus, human vision likely provides similar perception of the major colors in *D. pumilio* to that of avian predators.

ANCESTRAL CHARACTER STATE RECONSTRUCTION

We mapped dorsal coloration, ventral coloration, and spotting pattern onto a subtree containing the variable populations in the Bocas del Toro clade, using Puerto Viejo as a representative of the predominant Costa Rican morph, to root the tree. Because there are many methods of ancestral state character reconstruction and disagreement about which is best, we used both simple parsimony and stochastic character mapping, and performed each with the root fixed to characters fitting the predominant morph. For parsimony, we used MacClade version 4.0 (Maddison and Maddison 2000). For stochastic character mapping analysis, we used SIMMAP version 2.0 (Bollback 2006) with 10,000 draws from the prior distribution. Stochastic character mapping can be performed using a fully Bayesian approach that accommodates topological uncertainty and variation in model parameters by using Markov chain Monte Carlo (MCMC) samples from their respective posterior distributions. These distributions were drawn from the results of Bayesian phylogenetic analysis in MrBayes version 3.1.2 (Huelsenbeck and Ronquist 2001). In both approaches, we treated all characters as unordered and treated all transformations as equally probable.

HYPOTHESIS TESTING

Using a version of the SOWH test (Goldman et al. 2000; Swofford et al. 1996), we performed a parametric bootstrap analysis on different numbers of evolutionary changes to dull dorsal coloration and yellow ventral coloration. The SOWH test is a statistically robust tool for testing hypotheses of alternative tree topology (Shi et al. 2005) that is valuable in phylogenetic studies of trait evolution (Santos et al. 2003; Summers 2003). The method tests whether an ML phylogenetic tree estimated under a topological constraint is significantly worse than the optimal (unconstrained) tree. The probability of the observed difference in log-likelihood scores between the optimal tree (alternative) and the constrained tree (null) is evaluated by comparison against a distribution of differences in tree scores obtained from simulated datasets.

Because parametric bootstrapping with more than 15 taxa is prohibitively slow (Goldman et al. 2000), we reduced our dataset to single exemplars from each of the Bocas del Toro clade populations and retained one sample from Puerto Viejo as an outgroup. We compared our observed phylogenetic tree resulting from ML analysis to null hypothesis constraint trees with one to five changes to dull coloration. Under the single change tree, all dull-colored morphs were constrained to be an exclusive clade. For hypotheses of two to five changes, all possible combinations of constraint clades were evaluated and the shortest resulting tree was used (Santos et al. 2003). We repeated the same process with constraint trees corresponding to one, two, three, and four changes to yellow ventral coloration.

Finally, we tested our tree against a constraint tree for an a priori phylogeographic hypothesis corresponding to sequential vicariance of populations as islands were isolated in the Bocas del Toro archipelago (Fig. 3), based on the reconstruction of Anderson and Handley (2002). For this constraint tree, we excluded the island population Pastores and all mainland populations except Cerro Brujo because the historical estimates of island formation do not explicitly make predictions about these populations. The resulting tree took the form (((Colon, (Bastimentos, Solarte)), Agua), Popas, San Cristobal, Cerro Brujo) to represent the isolation of Colon, followed by Bastimentos + Solarte, followed by

Agua, and then by Popas and San Cristobal, from the peninsula on which Cerro Brujo is found. We did not constrain a root node because there is no a priori reason to expect rooting along a particular lineage and because a hypothesis tree with fewer constrained nodes is more difficult to reject (Fig. 3).

To perform the test, we calculated the test statistic by determining the −Ln likelihood difference between a given null hypothesis tree and the tree resulting from the observed data. We estimated the free parameters for the null tree topology from the observed data in PAUP* version 4.0b10 (Swofford 2001) and used these values to simulate 500 datasets on each of the null hypothesis trees using Seq-Gen version 1.3.2 (Rambaut and Grassly 1997). For each of the 500 simulated datasets, two ML trees were inferred, one without and one with the null constraint enforced, by heuristic ML searches starting from NJ trees and using TBR branch-swapping in PAUP* version 4.0b10 (Swofford 2001). The probability of correctly rejecting any null hypothesis was obtained by comparing our test statistic to the distribution of the difference in tree lengths obtained from the simulated data.

Results

PHYLOGENY

Sequencing resulted in a total of 3051 base pairs of mtDNA sequence data (685bp CytB, 640bp COI, 647bp ND4, 1079bp control region). Maximum-likelihood and Bayesian searches produced topologically identical trees (Fig. 4) with consistently high bootstrap values and posterior probabilities. Populations from Bocas del Toro did not form a monophyletic group. Although all but one of the island populations and mainland populations from Cerro Brujo, Guabo River, and Almirante did form a clade, mainland populations from Renacimiento and Uyama River and the island Escudo de Veraguas are not members of this clade. The Bocas del Toro clade will hereafter be referenced as including Colon, Bastimentos, Pastores, Almirante, San Cristobal, Cerro Brujo, Solarte, Guabo River, Popas, and Agua, as a way of distinguishing between this monophyletic group and the more inclusive set of geographical populations located in the Bocas del Toro region. Within the Bocas del Toro clade, populations were found to be monophyletic, with bootstrap values > 70 and posterior probabilities > 0.95 in all cases, except for Pastores, which is monophyletic with marginal statistical support (bootstrap $= 70$, posterior probability $= 0.92$) and Popas, which is weakly supported as paraphyletic with respect to a monophyletic Agua clade. These populations had an average pairwise sequence divergence of 1.08% (Table 4).

Results from the "minimize deep coalescences method" (Maddison and Knowles 2006) returned identical topological relationships to ML and Bayesian searches for the Bocas del Toro clade. Results for the relationships of the remaining populations differed only slightly, with samples from Renacimiento placed sister to Tortuguero rather than Bananito.

COLOR CLUSTERING

In 1000 replicates of k-means clustering, starting with centroids at randomly assigned points, the same two clusters were identified in 100% of trials for dorsal colors. These clusters corresponded to a red/orange cluster (Bastimentos, San Cristobal, Solarte, and Almirante) and a green/blue cluster (Colon, Pastores, Popas, Agua, Cerro Brujo, and Guabo River). For trials of $k = 3$, $k = 4$, and $k = 5$, identical clusters were only identified in 50.1%, 56.8% and 29.5% of trials, respectively. For ventral colors, clusters were most consistently identified when $k = 4$, with the same clusters appearing in 82.4% of replicates. These clusters corresponded to red (Solarte, San Cristobal, and Almirante), yellow (Colon, Popas, Agua, and Guabo River), green/blue (Pastores and Cerro Brujo), and white (Bastimentos). For trials of $k = 2$, $k = 3$, and $k = 5$, identical clusters were only identified in 54.5%, 66.7% and 31.0% of trials, respectively.

Results from clustering of spectral peaks support these color classes, with one exception. Dorsal spectral peaks clustered into two groups with wavelengths of approximately 530–555 nm (Colon, Pastores, Popas, and Guabo River) and 625–650 nm (Bastimentos, San Cristobal, Solarte, and Almirante). There was no clear spectral peak on any reflectance reading from the Cerro Brujo population, so we excluded this morph from dorsal clustering analysis. According to Summers et al. (2003), spectral peaks with wavelengths between 500 and 600 nm will appear green to yellow and those with wavelengths between 600 and 700 nm will appear orange to red, corresponding to the designations for clusters of RGB values. Ventral spectral peaks also clustered into four groups, corresponding to approximately 640–650 nm (Solarte, San Cristobal, and Almirante), 535–565 nm (Colon, Popas, Agua, Guabo River), 500 nm (Bastimentos), and 405 nm (Cerro Brujo). In each case, these clusters were recovered in 100% of trials. The sole difference between the two methods is the position of Pastores ventral coloration. The ventral coloration in this morph appears yellow-brown to human observers and was clustered with the blue coloration from Cerro Brujo based on digital imaging. Brown coloration is actually often the result of yellow pigmentation with low reflectance (Endler 1992). Digital images were not sensitive enough to detect this difference, as evidenced by the lower percentage of cluster recovery from these readings. However, spectrometer readings clearly indicate a spectral peak in the yellow wavelengths, and so we accept the clustering of Pastores with other yellow ventral color morphs for all remaining analyses. Otherwise, the high consistency of clusters identified with random starting points for $k = 2$ clusters in dorsal coloration and $k = 4$ clusters in ventral coloration offers strong support for distinct spatial clusters of color points in these traits, and

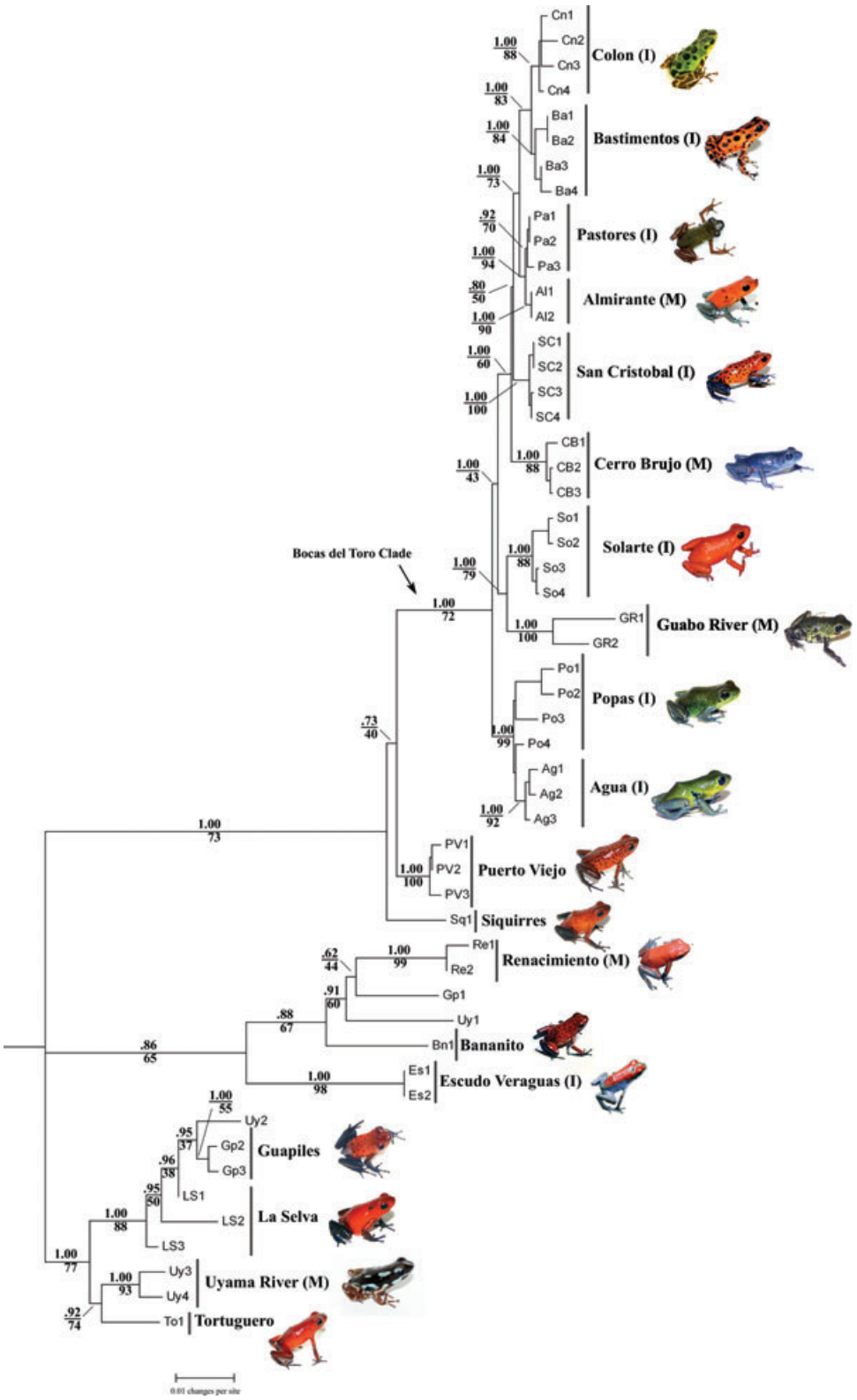

Figure 4. Maximum-likelihood (ML) phylogenetic tree for all known *Dendrobates pumilio* color morphs, based on 3051bp of mtDNA sequence data. ML Bootstrap values are indicated below each node; Bayesian posterior probabilities are indicated above each node. The names of island populations in Bocas del Toro are proceeded by an (I) and mainland populations in Bocas del Toro are proceeded by an (M).

Table 4. Nucleotide variation within and between populations. Values in bold along the diagonal represent within population variation. Net between population divergence estimates are below the diagonal (lower-left), and standard errors of net between population divergence are above the diagonal (upper-right). All calculations were performed in MEGA version 4.0.26 (Tamura et al. 2007). Acronyms correspond to those in Table 2 and Figures 3 and 4, and those representing populations in the Bocas del Toro clade are listed in bold.

	Ba	**So**	**Co**	**Pa**	**Po**	**CB**	**Ag**	**SC**	**Al**	**GR**	**PV**	Re	Uy	LS	Gp	Es	Bn	Sq	To
Ba	**0.003**	0.002	0.001	0.001	0.002	0.002	0.002	0.002	0.001	0.003	0.003	0.007	0.005	0.005	0.005	0.007	0.006	0.004	0.005
So	0.012	**0.004**	0.002	0.002	0.002	0.002	0.002	0.002	0.002	0.003	0.003	0.008	0.005	0.005	0.005	0.008	0.007	0.003	0.005
Co	0.002	0.012	**0.003**	0.001	0.002	0.002	0.002	0.002	0.001	0.003	0.003	0.007	0.005	0.005	0.005	0.007	0.006	0.004	0.005
Pa	0.005	0.012	0.005	**0.002**	0.002	0.001	0.002	0.001	0.001	0.003	0.003	0.008	0.005	0.005	0.005	0.007	0.006	0.004	0.005
Po	0.011	0.013	0.012	0.011	**0.003**	0.002	0.001	0.002	0.002	0.003	0.003	0.007	0.005	0.005	0.005	0.007	0.006	0.003	0.005
CB	0.010	0.014	0.010	0.010	0.014	**0.002**	0.002	0.002	0.002	0.003	0.003	0.008	0.005	0.005	0.005	0.007	0.006	0.004	0.005
Ag	0.012	0.012	0.012	0.011	0.002	0.015	**0.006**	0.002	0.002	0.003	0.003	0.007	0.005	0.005	0.005	0.007	0.006	0.003	0.005
SC	0.007	0.011	0.007	0.006	0.012	0.009	0.012	**0.001**	0.001	0.003	0.003	0.008	0.005	0.005	0.005	0.007	0.006	0.003	0.005
Al	0.005	0.012	0.005	0.002	0.011	0.010	0.009	0.006	**0.000**	0.003	0.003	0.008	0.005	0.005	0.005	0.007	0.006	0.004	0.005
GR	0.016	0.015	0.016	0.015	0.016	0.018	0.016	0.015	0.017	**0.016**	0.005	0.007	0.009	0.007	0.007	0.006	0.008	0.005	0.008
PV	0.024	0.025	0.023	0.024	0.023	0.025	0.020	0.025	0.025	0.033	**0.002**	0.007	0.005	0.005	0.005	0.008	0.006	0.002	0.005
Re	0.089	0.099	0.087	0.090	0.094	0.091	0.091	0.096	0.091	0.096	0.089	**0.003**	0.004	0.007	0.004	0.006	0.005	0.007	0.006
Uy	0.053	0.059	0.052	0.052	0.056	0.055	0.053	0.056	0.053	0.064	0.051	0.030	**0.045**	0.002	0.001	0.004	0.003	0.005	0.002
LS	0.069	0.072	0.069	0.069	0.069	0.071	0.069	0.072	0.068	0.080	0.060	0.061	0.008	**0.014**	0.002	0.007	0.005	0.005	0.003
Gp	0.056	0.061	0.055	0.055	0.058	0.057	0.055	0.058	0.056	0.063	0.054	0.030	0.036	0.007	**0.034**	0.004	0.003	0.005	0.003
Es	0.089	0.095	0.087	0.089	0.094	0.091	0.091	0.092	0.089	0.096	0.094	0.044	0.036	0.061	0.032	**0.000**	0.005	0.008	0.006
Bn	0.087	0.093	0.087	0.088	0.089	0.089	0.087	0.089	0.087	0.093	0.088	0.031	0.030	0.056	0.029	0.041	–	0.006	0.005
Sq	0.028	0.031	0.028	0.030	0.030	0.032	0.029	0.029	0.029	0.040	0.016	0.086	0.051	0.069	0.053	0.093	0.087	–	0.005
To	0.063	0.068	0.062	0.063	0.065	0.066	0.063	0.066	0.064	0.077	0.060	0.063	0.010	0.021	0.019	0.064	0.061	0.065	–

corroboration of results between the two clustering methods suggests that these represent visually distinct, discrete dorsal and ventral color classes.

Hereafter, we refer to the red/orange cluster of dorsal colors as the "bright" group and the blue/green cluster as the "dull" group, in keeping with other investigations of dendrobatid color groups (Roberts et al. 2006). Although the colors expressed in the bright group are typically associated with aposematism whereas the colors expressed in the dull group are commonly associated with crypsis, the extent to which the various colors displayed by color morphs in *D. pumilio* function as aposematic signals has not been extensively investigated. Although blue coloration has sometimes been invoked as aposematic, we include it in the dull group because of clustering results and observations (Summers et al. 2003) that the blue coloration of the Cerro Brujo morph appears dark compared to typical aposematic coloration. These designations are meant to represent the clusters only and are not meant to imply "brightness," "saturation," "percent reflectance," or other metrics sometimes used in measuring color.

ANCESTRAL STATE RECONSTRUCTION

Reconstructing characters onto our phylogenetic tree required multiple evolutionary transitions for all three aspects of color and pattern (Fig. 5). For dorsal coloration (Fig. 5A), both methods strongly supported bright coloration at all internal nodes except for the MRCA of Popas and Agua, which was dull under both methods. Both reconstructions suggest five independent changes from bright to dull coloration and no reversals to bright coloration. Character state reconstruction of ventral coloration and spotting pattern was more complicated. Ventral color reconstruction (Fig. 5B) required at least six changes. Both methods supported red ventral coloration at most internal nodes, with shifts to yellow in three lineages, blue in one lineage, and white in one lineage. Additionally, stochastic character mapping indicates a reversal from yellow to red in the Almirante lineage, although parsimony based reconstruction is equivocal for this branch. Spotting pattern (Fig. 5C) required five changes on the tree. The presence of large spots appears to have evolved only once, in the Bastimentos-Colon clade, but there were likely multiple shifts between solid and speckled patterns, probably in both directions.

HYPOTHESIS TESTING

SOWH tests support five changes to dull dorsal coloration. Null tree topologies with between one and four changes were each rejected ($P < 0.002$), but we were unable to reject the topology with five changes ($P = 1.0$). The five changes correspond to the Colon, Pastores, Cerro Brujo, Guabo River, and Popas + Agua lineages. SOWH tests also supported four changes to yellow ventral coloration. Null topologies for one, two, and three changes were each rejected ($P < 0.002$), but we were unable to reject the topology with four changes ($P = 1.0$). The four changes correspond to the Colon, Pastores, Guabo River, and Popas + Agua lineages. A SOWH test of the vicariance model of island isolation rejected the hypothesis that the relationships of populations in the Bocas del Toro archipelago are the result of the sequential island isolation depicted in Figure 3 ($P < 0.002$).

Discussion

Both color and pattern are expected to be tightly constrained in aposematic species (Harvey et al. 1982; Endler 1988; Darst and Cummings 2006; Reynolds and Fitzpatrick 2007). However, our mitochondrial results clearly demonstrate that color traits are extraordinarily labile in aposematic *D. pumilio*. Instead of a phylogenetically conservative history in which major changes in coloration occurred a minimal number of times, we find evidence for frequent shifts in coloration among the *D. pumilio* color morphs in Bocas del Toro, Panama, with multiple losses of bright dorsal coloration. The populations in this region also have a complex biogeographical history, which likely contributed to their diversification.

PHYLOGENY AND BIOGEOGRAPHY

Understanding the biogeographic history of any species relies on a sound, population-level phylogeny; ours is based on mitochondrial DNA. Phylogenetic results can be misleading when a gene tree conflicts with a population tree (Funk and Omland 2003; Rubinoff and Holland 2005). As a result, and because mtDNA may be more prone to introgression than nuclear DNA (Chan and Levin 2005), the value of mitochondrial DNA trees on their own has been the matter of much debate (Funk and Omland 2003; Rubinoff and Holland 2005; Zink and Barrowclough 2008). Clearly, there are certain limitations of using mtDNA to infer phylogenies, which make it unsuitable for some purposes (Funk and Omland 2003; Avise 2004; Rubinoff and Holland 2005). However, for inferring population history, mtDNA remains a valuable tool because of its high variability, rapid coalescence times, and sensitivity to recent population divergence, and should continue to be a robust marker for phylogeographic studies (Funk and Omland 2003; Avise 2004; Rubinoff and Holland 2005; Zink and Barrowclough 2008).

Three lines of evidence suggest that our mtDNA phylogeny of *D. pumilio* is likely a reasonable approximation of the true population tree. First, our results are broadly concordant with a recent nuclear AFLP analysis of these same populations (Rudh et al. 2007). They are not identical, but the similarity suggests that the single locus mtDNA analysis is not being badly compromised by selective sweeps or deep-coalescent historical processes. Second, Rudh et al. (2007) demonstrate that the Bocas del Toro populations are highly structured; they estimate global $F_{ST} = 0.232 \pm 0.015$, significant population structure ($F_{ST} > 0$) between all population

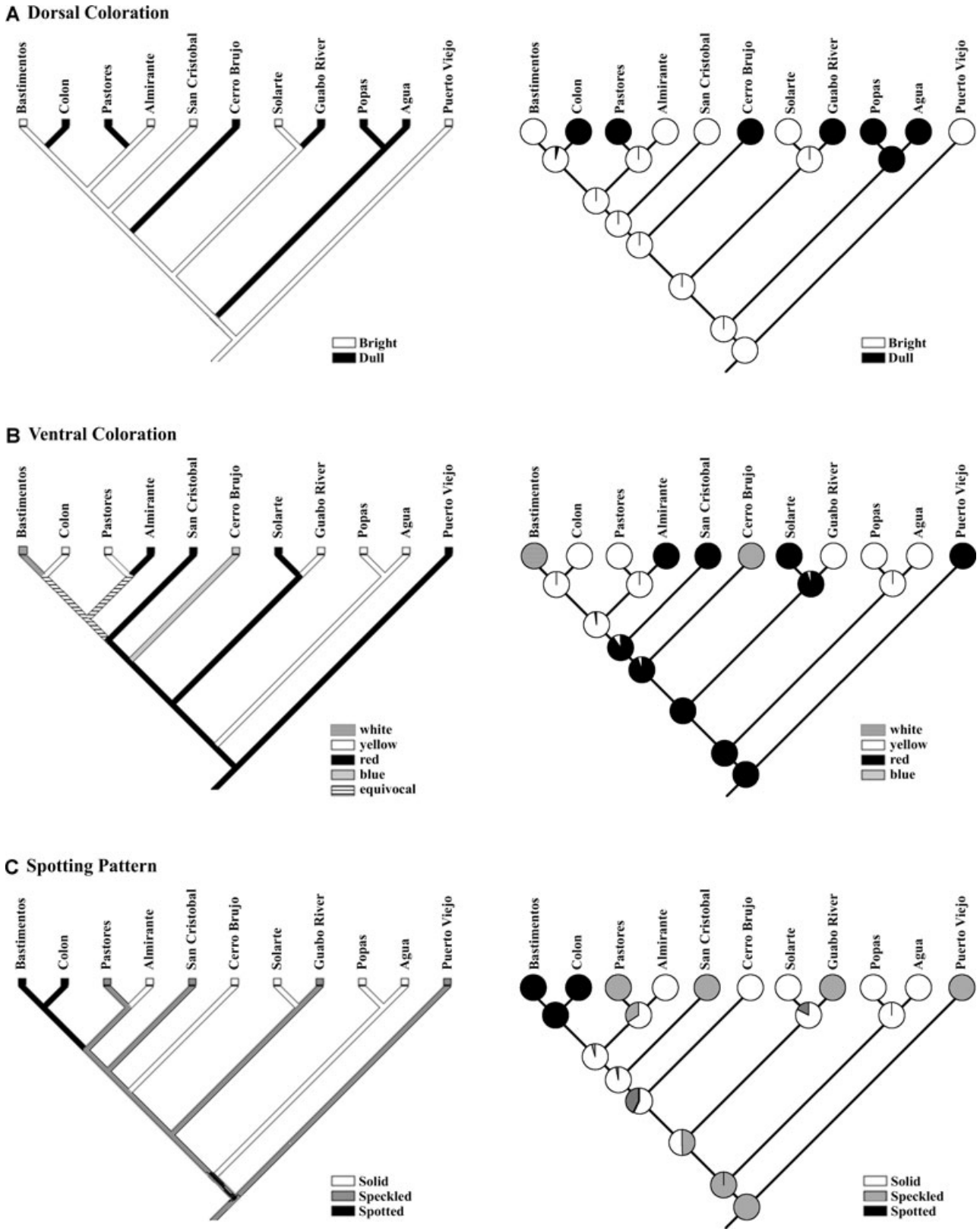

Figure 5. Ancestral state reconstruction of (A) dorsal coloration, (B) ventral coloration, and (C) spotting pattern for populations in the Bocas del Toro clade and with Puerto Viejo as an outgroup. We reconstructed ancestral states in two ways: (left) simple parsimony and (right) stochastic character mapping, both with a root fixed for the character state found in the predominant Costa Rican morph, represented by Puerto Viejo.

pairs, and an extremely low average interpopulation migration rate of 9.7×10^{-4} to 9.7×10^{-3}. Although this does not exclude the possibility of occasional gene flow, these data do indicate that populations in the Bocas del Toro clade have been evolving as independent units and that reticulate evolution between populations is unlikely. Finally, we sequenced three nuclear introns across the full range of Bocas del Toro populations for *D. pumilio* in an attempt to provide nuclear insights on population history, but found no phylogenetically informative sites among these populations in 2.1 kb of nuclear intron DNA sequences (I. J. Wang and H. B. Shaffer, unpubl. data). Although not informative, these data do conform to the low observed differentiation found for mtDNA (Table 4) and provide some evidence against the interpretation of introgression/selective sweeps as the reason for low mtDNA divergence.

Although our results are broadly consistent with previous mitochondrial and nuclear results, they also differ in important ways. The pioneering work of Summers et al. (1997) was based on a very short DNA fragment, and their analysis lacks the support to resolve most of the relationships among populations. Our results show some broad similarity to those of Hagemann and Prohl (2007). However, many phylogenetic details, including our finding of a sister group relationship of Bastimentos–Colon (rather than Bastimentos–Solarte and Colon–Pastores), and of Almirante–Pastores (instead of Almirante–San Cristobal), led us to a rather different conclusion regarding the evolution of both color pattern and phylogeographic history than Hagemann and Prohl (2007). The primary difference between the AFLP-based results of Rudh et al. (2007) and our analysis is that Bastimentos appears polyphyletic in their dendrogram, whereas it is monophyletic in ours with strong support (ML bootstrap = 84, Bayesian PP = 1.00); resolution of this discrepancy will require additional nuclear data. Our two studies are concordant in showing that some Bastimentos samples are sister to Colon and that San Cristobal and Cerro Brujo shared a common ancestor with each other more recently than either did with Popas, Agua, or Solarte. Further comparisons are difficult because of low bootstrap support for some nodes and the very sparse mainland sampling in Rudh et al.'s study.

Assuming then that our mitochondrial gene tree accurately reflects population history, our phylogeographic results indicate that the Bocas del Toro clade resulted from colonization by a lineage in Southeastern Costa Rica, most likely from Puerto Viejo. However, the invasion of the Bocas del Toro geographic region appears to have occurred multiple times. Populations from Escudo de Veraguas, Uyama River, and Renacimiento have different origins from the Bocas del Toro clade. The timing of these potential colonizations relative to that of the Bocas del Toro clade is not resolvable with our data, and there is no obvious biogeographic or time-dependent explanation for why one lineage (the Bocas del Toro clade) underwent a dramatic color-pattern radiation in this region whereas others did not.

Populations in the Bocas del Toro clade could have resulted from vicariance as islands became separated from the mainland, dispersal onto the islands after their isolation, or both. The SOWH test rejected the topology hypothesized by a strict vicariance model based on the known order of island isolation (Fig. 3), indicating that dispersal or preexisting differentiation played some role in generating the current population distribution. However, no clear dispersal pattern appears in the tree. Further confounding the analysis of island colonization are the positions of mainland populations relative to island populations. The presence of several island–mainland sister population pairs suggests multiple colonizations of the islands from mainland sources or from island to mainland, whereas island–island sister population pairs suggest additional among-island colonization. Thus, island to island, island to mainland, and mainland to island colonizations all likely played a role in generating the current distribution of these frogs.

A notable exception to the monophyletic structure of populations in the Bocas del Toro region is the population from Uyama River. Samples from this region occupy three separate positions in our phylogenetic tree. Along with Bastimentos, Uyama River is also one of the only populations showing substantial intrapopulation color polymorphism. Individuals from the Uyama River population have black dorsal coloration with two or three variable length stripes of light blue, yellow, or red (Fig. 1). If Uyama River is polyphyletic, then separate invasions by differentiated populations may explain the variation in color pattern. Alternatively, this population may not appear monophyletic because a much larger population previously existed, including this and nearby regions in Panama and much of Costa Rica, and insufficient time has passed for monophyly to evolve, even in the mitochondrial genome.

COLOR EVOLUTION

Six of the populations in the Bocas del Toro clade exhibit dull dorsal coloration, including shades of blue, green, and brown that are typically associated with crypsis. Dorsal coloration presumably plays a larger role than ventral coloration in aposematic signaling because avian (and most other) predators predominantly view these frogs from above (Siddiqi et al. 2004; Reynolds and Fitzpatrick 2007). Thus, changes in dorsal coloration may indicate shifts in predator avoidance strategy from aposematism to crypsis; future research should investigate the extent to which various colors function in *D. pumilio* in the wild. Cases of intraspecific polymorphism with both aposematic and cryptic morphs are sufficiently rare that they were long believed to not exist (Rubinoff and Kropach 1970; Edmunds 1974; Harvey et al. 1982). Evolutionary shifts away from aposematic coloration seem unlikely because individuals would abandon protective elements of their

phenotypes (Leimar et al. 1986), but there is little empirical or theoretical work to support this expectation.

Our results strongly support five separate changes to dull dorsal coloration in the Bocas del Toro populations of *D. pumilio*. SOWH tests rejected hypotheses of one, two, three, and four changes, and these results are supported by ancestral state reconstructions, which show that each of the five dully colored lineages was independently derived from a brightly colored ancestor. This finding is both unexpected and quite remarkable. Several explanations are consistent with the observed number of color changes in *D. pumilio*. Coloration in aposematic species may be a more labile trait than predicted, such that the predicted barriers to divergence are much less than expected. Alternatively, shifts from bright to dull coloration may be much more likely than shifts from dull to bright coloration. Finally, the constraints of normalizing selection on aposematic coloration may become relaxed if a population goes through a period of reduced toxicity, which may be more likely for species in which toxicity is dietarily induced. In this case, evolutionary forces, such as sexual selection or natural selection for local adaptation, may be enough to generate divergence (Summers et al. 1999; Gray and McKinnon 2007; Reynolds and Fitzpatrick 2007; Rudh et al. 2007).

We also find evidence for three or four separate changes to yellow ventral coloration. In addition to predator deterrence, the coloration in *D. pumilio* may be important in intraspecific signaling (Summers et al. 1999; Siddiqi et al. 2004; Reynolds and Fitzpatrick 2007). Color is known to play a role in male–female signaling, mate attraction, and male–male signaling in anurans (Summers et al. 1999; Hoffman and Blouin 2000; Reynolds and Fitzpatrick 2007). In these cases, ventral coloration may play a larger role than dorsal coloration. When signaling for mates, males enlarge their vocal sacs and posture on their front legs, revealing their ventral coloration. When contesting territories against invaders, males also present their ventral colors through similar posturing (Siddiqi et al. 2004; Reynolds and Fitzpatrick 2007). Thus, ventral coloration and dorsal coloration, which likely functions primarily for predator avoidance (Siddiqi et al. 2004; Reynolds and Fitzpatrick 2007), may be subject to substantially different forms of selection. One intriguing possibility is that relaxed selection for intense aposematic coloration allows for the differential expression of ventral coloration in response to intraspecific sexual selection.

Ancestral state reconstructions also indicate multiple shifts between dorsal spotting patterns across the phylogenetic tree. Spotting pattern may function as an independent signal, but may also enhance the effectiveness of other signals (Cott 1940; Endler 1992; Siddiqi et al. 2004; Hoekstra 2006). For instance, spotting pattern provides contrast to predominant colors in some species, making them more conspicuous, and breaks up regular patterns in others, making them more cryptic (Cott 1940). Overall, our results suggest the rapid evolution of novel phenotypes repeatedly driven by strong directional selection away from the ancestral red speckled phenotype; the next challenge is a more complete understanding of the functions of these color phenotypes.

CONVERGENT EVOLUTION

Our clustering results indicate a remarkable amount of convergence in dorsal and ventral coloration. Despite the wide range of color combinations in the Bocas del Toro clade, dorsal colors form distinct clusters. Dull dorsal coloration has evolved independently in five separate lineages, four of which have dorsal spectral reflectance peaks within a narrow range of wavelengths from 530 to 555 nm (we did not obtain a spectral peak measurement from Cerro Brujo). Additionally, four lineages have undergone independent changes to yellow ventral coloration. This indicates that evolution away from the ancestral red phenotype is nonrandom, and perhaps that dull green dorsal or yellow ventral coloration confers some adaptive advantage under the conditions experienced on certain islands. One possible explanation that has been considered is that reduced conspicuousness is associated with a reduction in toxicity (Daly and Myers 1967). However, although toxicity varies among the Bocas del Toro populations, it does not seem to be correlated with the brightness of coloration (Daly and Myers 1967). Another interesting consideration, presented by Summers et al. (2003), postulates that an ancestral green pigment synthesis pathway could have been modified to form other pigments in some populations and that frequent reversals could have occurred through relatively simple changes to that pathway. Unfortunately, both the genetic and physiological mechanisms underlying coloration in poison-dart frogs are poorly understood, and a close examination of pigment proteins and organelles remains an important area of research for understanding the properties of amphibian coloration (Summers et al. 2003).

CONCLUSIONS

Our results demonstrate that changes in coloration in aposematic species can, and do, occur repeatedly as independent events. This finding forces us to consider models for the evolution of aposematic coloration, the costs of gaining bright coloration versus losing it, developmental constraints on coloration, and the selective forces that could repeatedly drive shifts in coloration. The dramatic level of color polymorphism in the Bocas del Toro populations of *D. pumilio* remains difficult to explain, especially because our phylogeographic study of color evolution indicates a complex history of color changes. Our results also suggest that aposematic coloration based on environmentally induced toxicity may evolve in a fundamentally different way than that based on endogenously produced toxins, and we await additional comparative analyses of both types of aposematic systems.

ACKNOWLEDGMENTS

We thank A. Handzlik for providing tissues for preliminary analysis, and K. O'Connell and C. Wang for assistance in field collections. We thank the Shaffer lab group and a UC Davis Monte Carlo group for advice on the project. We are grateful to the environmental authorities in Panama (ANAM) and Costa Rica (MINAE) for granting scientific collection permits and to O. Acevedo at the Smithsonian Tropical Research Institute and F. Campos at the Organization for Tropical Studies for assistance in obtaining them. This work was supported by the UC Davis Center for Population Biology and an NSF Graduate Research Fellowship (to IJW) and by the NSF (DEB 0516475, DEB 0213155) and the UC Davis Agricultural Experiment Station (to HBS) and was conducted in partial fulfillment of IJW's Ph.D. dissertation.

LITERATURE CITED

Abramoff, M. D., P. J. Magelhaes, and S. J. Ram. 2004. Image processing with ImageJ. Biophotonics Intl. 11:36–43.

Anderson, R. P., and J. C. O. Handley. 2002. Dwarfism in insular sloths: biogeography, selection, and evolutionary rate. Evolution 56:1045–1058.

Arevalo, E., S. K. Davis, and J. W. Sites, Jr. 1994. Mitochondrial DNA sequence divergence and phylogenetic relationships among eight chromosome races of the *Sceloporus grammicus* complex (Phrynosomatidae) in central Mexico. Syst. Biol. 43:387–418.

Avise, J. C. 2004. Molecular markers, natural history, and evolution. Sinauer Assoc., Sunderland, MA.

Benson, W. W. 1972. Natural selection for Mullerian mimicry in *Heliconius erato* in Costa Rica. Science 26:936–939.

Bollback, J. P. 2006. SIMMAP: stochastic character mapping of discrete traits on phylogenies. BMC Bioinformatics 7:1–7.

Burns, E., M. Eldridge, D. Crayn, and B. Houlden. 2007. Low phylogeographic structure in a wide spread endangered Australian frog *Litoria aurea* (Anura: Hylidae). Conserv. Genet. 8:17–32.

Chan, K. M. A., and S. A. Levin. 2005. Leaky prezygotic isolation and porous genomes: rapid introgression of maternally inherited DNA. Evolution 49:720–729.

Cott, H. B. 1940. Adaptive coloration in animals. Methuen, London.

Crawford, A. J., E. Bermingham, and P. S. Carolina. 2007. The role of tropical dry forest as a long-term barrier to dispersal: a comparative phylogeographical analysis of dry forest tolerant and intolerant frogs. Mol. Ecol. 16:4789–4807.

Daly, J. W., and C. W. Myers. 1967. Toxicity of Panamanian poison frogs (*Dendrobates*): some biological and chemical aspects. Science 156:970–973.

Darst, C. R., and M. E. Cummings. 2006. Predator learning favours mimicry of a less-toxic model in poison frogs. Nature 440:208–211.

Edmunds, M. 1974. Defence in animals: a survey of anti-predator defences. Longman, London.

Endler, J. A. 1988. Frequency-dependent predation, crypsis and aposematic coloration. Philos. Trans. R. Soc. Lond. B 319:505–523.

———. 1992. Signals signal conditions and the direction of evolution. Am. Nat. 139:125–153.

Endler, J., and J. Mappes. 2004. Predator mixes and the conspicuousness of aposematic Signals. Am. Nat. 163:532–547.

Endler, J. A., and P. W. Mielke. 2005. Comparing entire colour patterns as birds see them. Biol. J. Linn. Soc. 86:405–431.

Felsenstein, J. 1981. Evolutionary trees from DNA sequences: a maximum likelihood approach. J. Mol. Evol. 17:368–376.

———. 1985. Confidence limits on phylogenies: an approach using the bootstrap. Evolution 39:783–791.

Folmer, O., M. Black, W. Hoeh, R. Lutz, and R. Vrijenhoek. 1994. DNA primers for amplification of mitochondrial cytochrome c oxidase subunit I from diverse metazoan invertebrates. Mol. Mar. Biol. Biotech. 3:294–299.

Funk, D. J., and K. E. Omland. 2003. Species-level paraphyly and polyphyly: frequency, causes, and consequences, with insights from animal mitochondrial DNA. Annu. Rev. Ecol. Evol. Syst. 34:397–423.

Goebel, A. M., J. M. Donnelly, and M. E. Atz. 1999. PCR primers and amplification methods for 12S ribosomal DNA, the control region, cytochrome oxidase I, and cytochrome b in bufonids and other frogs, and an overview of PCR primers which have amplified DNA in amphibians successfully. Mol. Phylogenet. Evol. 11:163–199.

Goldman, N., J. P. Anderson, and A. G. Rodrigo. 2000. Likelihood-based tests of topologies in phylogenetics. Syst. Biol. 49:652–670.

Gordon, A. 1999. Classification. Chapman and Hall, London.

Grant, T., D. R. Frost, J. P. Caldwell, R. Gagliardo, C. F. B. Haddad, P. J. R. Kok, D. B. Means, B. P. Noonan, W. R. Schargel, and W. C. Wheeler. 2006. Phylogenetic systematics of dart-poison frogs and their relatives (Amphibia: Athesphatanura: Dendrobatidae). B. Am. Mus. Nat. Hist. 299:1–262.

Gray, S. M., and J. S. McKinnon. 2007. Linking color polymorphism maintenance and speciation. Trends Ecol. Evol. 22:71–79.

Guilford, T., and M. S. Dawkins. 1993. Are warning colors handicaps? Evolution 47:400–416.

Hagemann, S., and H. Prohl. 2007. Mitochondrial paraphyly in a polymorphic poison frog species (Dendrobatidae; *D. pumilio*). Mol. Phylogenet. Evol. 45:740–747.

Hartigan, J. A., and M. A. Wong. 1979. A k-means clustering algorithm. Appl. Stat. 28:100–108.

Harvey, P. H., J. J. Bull, M. Pemberton, and R. J. Paxton. 1982. The evolution of aposematic coloration in distasteful prey: a family model. Am. Nat. 119:710–719.

Hoekstra, H. E. 2006. Genetics, development and evolution of adaptive pigmentation in vertebrates. Heredity 97:222–234.

Hoffman, E. A., and M. S. Blouin. 2000. A review of colour and pattern polymorphisms in anurans. Biol. J. Linn. Soc. 70:633–665.

Huelsenbeck, J. P., and F. Ronquist. 2001. MRBAYES: Bayesian inference of phylogenetic trees. Bioinformatics 17:754–755.

Joron, M., I. Wynne, G. Lamas, and J. Mallet. 1999. Variable selection and the coexistence of multiple mimetic forms of the butterfly *Heliconius numata*. Evol. Ecol. 13:721–754.

Knowles, L. L., and B. C. Carstens. 2007. Estimating a geographically explicit model of population divergence. Evolution 61:477–493.

Leimar, O., M. Enquist, and B. Sillen-Tullberg. 1986. Evolutionary stability of aposematic coloration and prey unprofitability: a theoretical analysis. Am. Nat. 128:469–490.

Maddison, W. P., and L. L. Knowles. 2006. Inferring phylogeny despite incomplete lineage sorting. Syst. Biol. 55:21–30.

Maddison, D. R., and W. P. Maddison. 2000. MacClade: analysis of phylogeny and character evolution. Sinauer Assoc., Sunderland, MA.

Maddison, W. P., and D. R. Maddison. 2005. MESQUITE: A Modular System for Evolutionary Analysis. Available: http://www.mesquiteproject.org.

Mallet, J., and M. Joron. 1999. Evolution of diversity in warning color and mimicry: polymorphisms, shifting balance, and speciation. Evolution 30:201–233.

Merilaita, S., and B. S. Tullberg. 2005. Constrained camouflage facilitates the evolution of conspicuous warning coloration. Evolution 59: 38–45.

Muller, F. 1879. *Ituna* and *Thyridia*: a remarkable case of mimicry in butterflies. Proc. Entom. Soc. Lond. 1879:20–29.

Myers, C., and J. Daly. 1983. Dart-poison frogs. Sci. Am. 248:120–133.

Norris, K. S., and C. H. Lowe. 1964. An analysis of background color-matching in amphibians and reptiles. Ecology 45:565–580.

Olson, S. L. 1993. Contributions to avian biogeography from the archipelago and lowlands of Bocas del Toro, Panama. Auk 110:100–108.

Posada, D., and K. A. Crandall. 1998. Modeltest: testing the model of DNA substitution. Bioinformatics 14:817–818.

Puurtinen, M., and V. Kaitala. 2006. Conditions for the spread of conspicuous warning signals: a numerical model with novel insights. Evolution 60:2246–2256.

Rambaut, A., and N. C. Grassly. 1997. Seq-Gen: an application for the Monte Carlo simulation of DNA sequence evolution along phylogenetic trees. Comp. Appl. Biosci. 13:235–238.

Rannala, B., and Z. Yang. 1996. Probability distribution of molecular evolutionary trees: a new method of phylogenetic inference. J. Mol. Evol. 43:304–311.

Reynolds, R. G., and B. M. Fitzpatrick. 2007. Assortative mating in poison-dart frogs based on an ecologically important trait. Evolution 61:2253–2259.

Roberts, J. L., J. L. Brown, R. von May, W. Arizabal, R. Schulte, and K. Summers. 2006. Genetic divergence and speciation in lowland and montane Peruvian poison frogs. Mol. Phylogenet. Evol. 41:149–164.

Rowe, C., and T. Guilford. 2000. Aposematism: to be red or dead. Trends Ecol. Evol. 15:261–262.

Rubinoff, D., and B. S. Holland. 2005. Between two extremes: mitochondrial DNA is neither the panacea nor the nemesis of phylogenetic and taxonomic inference. Syst. Biol. 54:952–961.

Rubinoff, I., and C. Kropach. 1970. Differential reactions of Atlantic and Pacific predators to sea snakes. Nature 228:1288–1290.

Rudh, A., B. Rogell, and J. Hoglund. 2007. Non-gradual variation in colour morphs of the strawberry poison frog *Dendrobates pumilio*: genetic and geographical isolation suggest a role for selection in maintaining polymorphism. Mol. Ecol. 20:4284–4294.

Saitou, N., and M. Nei. 1987. The neighbor-joining method: a new method for reconstructing phylogenetic trees. Mol. Biol. Evol. 4:406–425.

Santos, J., L. A. Coloma, and D. C. Cannatella. 2003. Multiple, recurring origins of aposematism and diet specialization in poison frogs. Proc. Natl. Acad. Sci. USA 100:12792–12797.

Saporito, R. A., H. M. Garraffo, M. A. Donnelly, A. L. Edwards, J. T. L. Longino, and J. W. Daly. 2004. Formicine ants: an arthropod source for the pumiliotoxin alkaloids of dendrobatid poison frogs. Proc. Natl. Acad. Sci. USA 101:8045–8050.

Saporito, R. A., R. Zuercher, M. Roberts, K. G. Gerow, and M. A. Donnelly. 2007. Experimental evidence for aposematism in the dendrobatid poison frog *Oophaga pumilio*. Copeia 25:1006–1011.

———. 2002. The amphibians and reptiles of Costa Rica: a herpetofauna between two continents, between two seas. The Univ. of Chicago Press, Chicago, IL.

Servedio, M. R. 2000. The effects of predator learning, forgetting, and recognition errors on the evolution of warning coloration. Evolution 54:751–763.

Shi, X., H. Gu, E. Susko, and C. Field. 2005. The comparison of the confidence regions in phylogeny. Mol. Biol. Evol. 22:2285–2296.

Siddiqi, A., T. W. Cronin, E. R. Loew, M. Vorobyev, and K. Summers. 2004. Interspecific and intraspecific views of color signals in the strawberry poison frog *Dendrobates pumilio*. J. Exp. Biol. 207:2471–2485.

Speed, M. P., and G. D. Ruxton. 2005. Aposematism: what should our starting point be? Proc. R. Soc. Lond. B 272:431–438.

Stevens, M., C. A. Parraga, I. C. Cuthill, J. C. Partridge, and T. S. Troscianko. 2007. Using digital photography to study animal coloration. Biol. J. Linn. Soc. 90:211–237.

Summers, K. 2003. Convergent evolution of bright coloration and toxicity in frogs. Proc. Natl. Acad. Sci. USA 100:12533–12534.

Summers, K., and M. E. Clough. 2001. The evolution of coloration and toxicity in the poison frog family (Dendrobatidae). Proc. Natl. Acad. Sci. USA 98:6227–6232.

Summers, K., E. Bermingham, L. Weigt, S. McCafferty, and L. Dahlstrom. 1997. Phenotypic and genetic divergence in three species of dart-poison frogs with contrasting parental behavior. J. Hered. 88:8–13.

Summers, K., R. Symula, M. Clough, and T. Cronin. 1999. Visual mate choice in poison frogs. Proc. R. Soc. Lond. B 266:2141–2145.

Summers, K., T. W. Cronin, and T. Kennedy. 2003. Variation in spectral reflectance among populations of *Dendrobates pumilio*, the strawberry poison frog, in the Bocas del Toro archipelago, Panama. J. Biogeogr. 30:35–53.

Summers, K., T. Cronin, and T. Kennedy. 2004. Cross-breeding of distinct color morphs of the strawberry poison frog (*Dendrobates pumilio*) from the Bocas del Toro archipelago, Panama. J. Herp. 38:1–8.

Swofford, D. L. 2001. PAUP*: Phylogenetic Analysis Using Parsimony (*and Other Methods), version 4.0. Sinauer, Sunderland, MA.

Swofford, D. L., G. J. Olsen, P. J. Waddell, and D. M Hillis. 1996. Phylogenetic inference. Pp. 407–514 *in* D. M. Hillis, C. Moritz, B. K. Mable, eds. Molecular systematics. Sinauer, Sunderland, MA.

Tamura, K., and M. Nei. 1993. Estimation of the number of nucleotide substitutions in the control region of mitochondrial DNA in humans and chimpanzees. Mol. Biol. Evol. 10:512–526.

Tamura, K., J. Dudley, M. Nei, and S. Kumar. 2007. MEGA4: Molecular Evolutionary Genetics Analysis (MEGA) software version 4.0. Mol. Biol. Evol. 24:1596–1599.

Tibshirani, R., G. Walther, and T. Hastie. 2001. Estimating the number of clusters in a data set via the gap statistic. J. R. Stat. Soc. B 63:411–423.

Vences, M., J. Kosuch, R. Boistel, C. F. B. Haddad, E. La Marca, S. Lotters, and M. Veith. 2003. Convergent evolution of aposematic coloration in Neotropical poison frogs: a molecular phylogenetic perspective. Org. Div. Evol. 3:215–226.

Vorobyev, M., D. Osorio, A. T. D. Bennett, N. J. Marshall, and I. C. Cuthill. 1998. Tetrachromacy, oil droplets and bird plumage colours. J. Comp. Physiol. A 183:621–633.

Wang, I. J., A. J. Crawford, and E. Bermingham. 2008. Phylogeography of the pygmy rain frog (*Pristimantis ridens*) across the lowland wet forests of isthmian central America. Mol. Phylogenet. Evol. 47:992–1004.

Yachi, S., and M. Higashi. 1998. The evolution of warning signals. Nature 394:882–884.

Yang, Z., and B. Rannala. 1997. Bayesian phylogenetic inference using DNA sequences: a Markov chain Monte Carlo method. Mol. Biol. Evol. 14:717–724.

Zink, R. M., and G. F. Barrowclough. 2008. Mitochondrial DNA under siege in avian phylogeography. Mol. Ecol. 17:2107–2121.

Associate Editor: H. Hoekstra